Clinical Cancer Research

Targeting Purinergic Receptor P2Y2 Prevents the Growth of Pancreatic Ductal Adenocarcinoma by Inhibiting Cancer Cell Glycolysis

Li-Peng Hu[1], Xiao-Xin Zhang[2], Shu-Heng Jiang[2], Ling-Ye Tao[3], Qing Li[2], Li-Li Zhu[1], Ming-Wei Yang[3], Yan-Miao Huo[3], Yong-Sheng Jiang[3], Guang-Ang Tian[2], Xiao-Yan Cao[2], Yan-Li Zhang[2], Qin Yang[2], Xiao-Mei Yang[2], Ya-Hui Wang[2], Jun Li[2], Gary Guishan Xiao[4,5], Yong-Wei Sun[3], and Zhi-Gang Zhang[1,2]

Abstract

Purpose: Extensive research has reported that the tumor microenvironment components play crucial roles in tumor progression. Thus, blocking the supports of tumor microenvironment is a promising approach to prevent cancer progression. We aimed to determine whether blocking extracellular ATP–P2RY2 axis could be a potential therapeutic approach for PDAC treatment.

Experimental Design: Expression of P2RY2 was determined in 264 human PDAC samples and correlated to patient survival. P2RY2 was inhibited in human PDAC cell lines by antagonist and shRNA, respectively, and cell viability, clonogenicity, and glycolysis were determined. RNA sequencing of PDAC cell line was applied to reveal underlying molecular mechanisms. Multiple PDAC mouse models were used to assess the effects of the P2RY2 inhibition on PDAC progression.

Results: P2RY2 was upregulated and associated with poor prognosis in PDAC. Activated P2RY2 by increased extracellular ATP in tumor microenvironment promoted PDAC growth and glycolysis. Further studies showed that the agonist-activated P2RY2 triggered PI3K/AKT–mTOR signaling by crosstalk with PDGFR mediated by Yes1, resulting in elevated expression of c-Myc and HIF1α, which subsequently enhanced cancer cell glycolysis. Genetic and pharmacologic inhibition of P2RY2 impaired tumor cell growth in subcutaneous and orthotopic xenograft model, as well as delayed tumor progression in inflammation-driven PDAC model. In addition, synergy was observed when AR-C118925XX, the selective antagonist of P2RY2 receptor, and gemcitabine were combined, resulting in prolonged survival of xenografted PDAC mice.

Conclusions: These findings reveal the roles of the P2RY2 in PDAC metabolic reprogramming, suggesting that P2RY2 might be a potential metabolic therapeutic target for PDAC.

Introduction

Pancreatic ductal adenocarcinoma (PDAC) is one of the most lethal human cancers with a 5-year survival rate of approximately 8% (1). Despite much efforts have been invested, there is still no effective drug available for therapy of the disease, and the prognosis of PDAC has shown less improvement in decades (2, 3). It is thus an unmet need for understanding of the mechanism underlying regulation of PDAC to develop effective targets for therapy of PDAC.

Many studies have reported that the tumor microenvironment, including the cellular and noncellular components of the tumor niche, plays a critical role in tumor progression (4). Cancer cells form intimate associations with stromal cells, resulting in an aberrant increase in growth factors (5), cytokines (6), chemokines (7), and metabolites (8) within the tumor microenvironment. The receptors and transporters activated by extracellular proteins or metabolites create the crosstalk between cancer and stromal cells, which results in metabolic reprograming in the microenvironment, leading to the reduced immune response and the accelerated growth of cancer cell, and eventually apoptosis escaped. Therefore, abolishing the extracellular supports from the tumor microenvironment may be a promising approach for effective therapy of cancer.

G-protein–coupled receptors (GPCR), the largest transmembrane receptor family in humans, are critical responders of extracellular stimulation and modulators of intracellular signaling pathways (9). It is well established that GPCRs are

[1]State Key Laboratory of Oncogenes and Related Genes, Ren Ji Hospital, School of Biomedical Engineering, Shanghai Jiao Tong University, Shanghai, P.R. China. [2]State Key Laboratory of Oncogenes and Related Genes, Shanghai Cancer Institute, Ren Ji Hospital, School of Medicine, Shanghai Jiao Tong University, Shanghai, P.R. China. [3]Department of Biliary-Pancreatic Surgery, Ren Ji Hospital, School of Medicine, Shanghai Jiao Tong University, Shanghai, P.R. China. [4]School of Pharmaceutical Science and Technology, Dalian University of Technology, Dalian, P.R. China. [5]Functional Genomics and Proteomics Laboratory, Osteoporosis Research Center, Creighton University Medical Center, Omaha, Nebraska.

Note: Supplementary data for this article are available at Clinical Cancer Research Online (http://clincancerres.aacrjournals.org/).

L.-P. Hu, X.-X. Zhang, and S.-H. Jiang contributed equally to this article.

Corresponding Authors: Zhi-Gang Zhang, Shanghai Cancer Institute, Ren Ji Hospital, Shanghai Jiao Tong University School of Medicine, Shanghai Jiao Tong University, 800 Dongchuan Road, Shanghai 200240, P.R. China. Phone: 8621-3420-6763; Fax: 8621-3420-6022; E-mail: zzhang@shsci.org; Yong-Wei Sun, syw0616@126.com; and Gary Guishan Xiao, School of Pharmaceutical Science and Technology, Dalian University of Technology. E-mail: gxiao@dlut.edu.cn

doi: 10.1158/1078-0432.CCR-18-2297

Translational Relevance

Tumor microenvironment is widely reported to be involved in cancer progression. Abolishing the supports from tumor microenvironment components would be an effective way to prevent cancer progression. Our study revealed that increased extracellular ATP in pancreatic ductal adenocarcinoma (PDAC) microenvironment promotes cancer progression by activating Purinergic Receptor P2Y2 (P2RY2). Thus, activated P2RY2 resulted in activation of PI3K–mTOR pathway and elevation of cancer glycolysis by crosstalk with PDGFRβ, as intermediated by Src family kinase, Yes1. Blocking P2RY2 by a selective inhibitor AR-C 118925XX profoundly suppressed tumor progression, prolonged orthotopic PDAC mice survival, and exhibited synergistic effect with gemcitabine. Together, P2RY2 might be a promising target for PDAC therapy.

crucial mediators in the communication between cancer cells and other components in the microenvironment (10–12). In addition, GPCRs are critical pharmaceutical acceptable targets for the treatment of diseases (13), which may also presumably hold true for PDAC.

Here, we aimed to identify novel therapeutic targets for PDAC. We found that P2RY2 expression was elevated in PDAC and its high expression correlated with poor survival in patients with PDAC. Further studies revealed that activated P2RY2 promoted cancer progression by enhanced glycolysis. Genetic or pharmacologic inhibition of P2RY2 significantly suppressed PDAC cell growth both *in vitro* and *in vivo*. Collectively, our results indicate that targeting P2RY2 may provide a new opportunity for PDAC therapy.

Materials and Methods

Seahorse analyses

The assays for extracellular acidification rate (ECAR) and oxygen consumption rate (OCR) in the cultured cells were performed with the Seahorse XF96 Flux Analyzer (Seahorse Bioscience, Agilent) according to the manufacturer's instructions. Briefly, AsPC-1 and BxPC-3 cells were seeded in a XF96-well plate at a density of 1×10^4 per well with the indicated treatment. The media were replaced with assay media at 1 hour before the assay. For the glycolytic stress test (Seahorse Bioscience, catalog no. 103020-100), 10 mmol/L glucose, 1 μmol/L oligomycin, and 50 mmol/L 2-deoxyglucose (2-DG) were injected to the wells. For the mitochondrial stress test (Seahorse Bioscience, catalog no. 103015-100), 1 μmol/L oligomycin, 1 μmol/L FCCP, 0.5 μmol/L rotenone, and 0.5 μmol/L actinomycin A were added to the wells. Both measurements were normalized by total protein quantitation. The experiments mentioned above were performed in triplicate and repeated twice.

Glucose and lactate measurement

Cells were grown in 24-well plate culture dishes overnight, followed by treating with indicated antagonists for 2 hours, and then stimulated with ATP (20 μmol/L) for an additional 24 hours. The culture media were clarified by centrifugation and the supernatants were filtered with 0.22-μm filters used for the measurement of glucose and lactate concentration. Total protein was extracted from the cell pellets and quantified by Bradford (Thermo Fisher Scientific, catalog no. 23227). Glucose uptake was measured using Amplex Red Glucose/Glucose Oxidase Assay Kit (Invitrogen, catalog no. A22189). Glucose consumption was calculated by the net content of the original glucose concentration deduced from the measured glucose concentration in the medium. Lactate production was measured by using the Lactate Assay Kit (BioVision, catalog no. ABIN411683). Total proteins were used for normalization of the results obtained above. These experiments were performed in triplicate manner and repeated twice.

Extracellular ATP measurement

The ATP levels were determined using a bioluminescent ATP Assay Kit (Beyotime, catalog no. S0027) according to the manufacturer's instructions. Tumor interstitial fluids were collected as reported previously (14). Briefly, tissues were supported with triple-layered 10-μm nylon mesh in the tube and centrifuged at $50 \times g$ for 5 minutes to remove surface liquids of tissues, followed by centrifugation at $400 \times g$ for another 10 minutes to collect interstitial fluids. The ectonucleotidase inhibitor ARL 67156 trisodium salts were added to the tumor interstitial fluid throughout the procedure. Luminescence was measured using a luminometer (M1000 PRO, TECAN). The standard ATP samples were used for preparation of the calibration curve. Results were normalized by total protein from each sample. All experiments were performed in triplicate and repeated twice.

Human PDAC tissue array analysis

The study was conducted in accordance with International Ethical Guidelines for Biomedical Research Involving Human Subjects (CIOMS). The study was approved by the Research Ethics Committee of Ren Ji Hospital, School of Medicine, Shanghai Jiao Tong University (Shanghai, P.R. China). Written informed consent was provided to all the patients before enrollment. The patient cohort of human pancreatic tissue array containing 264 PDAC specimens and corresponding noncancerous tissues were also obtained from Ren Ji Hospital (Shanghai Jiao Tong University School of Medicine, Shanghai, P.R. China) from January 2002 to June 2015. Patients had not received radiotherapy, chemotherapy, or other related antitumor therapies before surgery. Before surgery, none of the patients had received antitumor therapies. The tissue staining was scored 0 when < 5% tumor cells showed expression. Positive scores (1–3) were based on percent of tumor cells and staining intensity within the tumor sample.

Animal model studies

Animal experiments were approved by Institutional Animal Care and Use Committee of East China Normal University (Shanghai, P.R. China). Mice were manipulated and housed according to the criteria outlined in the Guide for the Care and Use of Laboratory Animals prepared by the National Academy of Sciences and published by the NIH (Bethesda, MD).

Subcutaneous and orthotopic xenograft model

Athymic male nu/nu mice aged from 6 to 8 weeks were used in this study. Subcutaneous implant models were established by subcutaneous injection at a total cell number of 2×10^6 for

either shNC or shP2RY2 AsPC-1 cells in 100 μL RPIM1640 in the right back flank of mice. Tumor diameters were monitored with calipers every three days. Mice were sacrificed after 30 days and the tumor was isolated and weighed. For pharmacologic study in subcutaneous xenografts, a total of 2×10^6 cells either AsPC-1 cells or BxPC-3 in 100 μL RPIM1640 were injected subcutaneously into the lower back. When tumors were borne (200 mm^3), animals were randomly divided into two groups (Ctrl and AR-C). Mice in AR-C group were given intraperitoneal injection of AR-C at10 mg/kg every 5 days, while Ctrl group was treated with 100 μL 0.9% NaCl. Tumor volumes were calculated by volume $= 0.5 \times$ length $\times$ width^2. For orthotopic xenografts study, 1×10^6 luciferase-expressing Panc 02 cells suspended in 25 μL DMEM were transplanted into the body of pancreas. Mice were randomly divided into four groups treated with 0.9% NaCl, AR-C (10 mg/kg), gemcitabine (50 mg/kg), and AR-C plus gemcitabine for four weeks after 5 days postsurgery, respectively. Luciferin emission imaging of isoflurane-anesthetized animals was measured every 5 days using the IVIS Spectrum (Caliper Life Sciences) after intraperitoneal injection of D-luciferin (150 mg; Promega, catalog no. P1043,) into the mice. Five mice from each group were chosen randomly for bioluminescent imaging. Emission was quantified using Living Image software, version 4.5.3.

PDAC transgenic model

PDAC transgenic mouse model used in this study was generated by crossing Pdx1-Cre mice onto lox-stop-lox-Kras$^{G12D/+}$ and lox-stop-loxTrp53$^{R172H/+}$ (KPC). A cohort of lox-stop-lox-Kras$^{G12D/+}$; Pdx1-Cre (KC) mice was used to generate pancreatic inepithelial neoplasia lesions (PanIN). KPC mice pancreas tissues were collected when they bore touchable tumors. Eighteen-week-old and 36-week-old KC mice were sacrificed to collect early and late PanIN lesion–contained pancreas.

Inflammation-driven PDAC model

Inflammation-driven PDAC model was generated as reported previously (15). Briefly, KC mice at the age of 9–10 weeks were fasted overnight, following six hourly intraperitoneal injections of cerulein (HY-A0190, MCE; 50 mg/kg) in 48 consecutive hours. Mice were randomly divided into two groups (3 mice/group) after the last dose of cerulein and then AR-C (10 mg/kg) or 0.9% NaCl was injected every five days for another 10 weeks and sacrificed.

Statistical analysis

All statistics were carried out using GraphPad Prism 7.0 and Excel. After testing for normal distribution, statistical analysis was performed using ANOVA when more than two groups were compared, two-way ANOVA when two conditions were investigated, and a two-tailed Students *t* test when only two groups of data were concerned. Comparison of Kaplan–Meier survival curves was performed with the log-rank Mantel–Cox test. All experiments with cell lines were done in at least triplicates. All error bars in this study represent the mean ± SD, except for bioluminescent emission, whose error bars represent the mean ± SEM (n.s, $P > 0.05$; *, $P \leq 0.05$; **, $P \leq 0.01$; ***, $P \leq 0.001$).

Additional information and associated materials are available in Supplementary Materials and Methods.

Results

P2RY2 expression is correlated with poor prognosis in PDAC

To explore potential GPCR therapeutic targets for PDAC, we first analyzed the expression of GPCRs in the following three GEO datasets: GSE16515, GSE28735, and GSE102238. The results showed that 37 GPCRs (Supplementary Table S1) were upregulated in cancer tissues compared with the corresponding adjacent nontumor tissues (Fig. 1A). We then investigated the clinical relevance of these GPCRs using the TCGA database and found that only three of them, namely, P2RY2, GPR39, and GPRC5A, positively correlated with a poor prognosis in PDAC (Fig. 1B; Supplementary Fig. S1A). As GPR39 and GPRC5A are orphan receptors, we focused on P2RY2, a receptor for ATP and UTP. To validate the clinical relevance of P2RY2 in PDAC, we detected the expression pattern of P2RY2 in mouse and human PDAC tissues. IHC results from genetically engineered mouse model of LSL-Kras$^{G12D/+}$; LSL-Trp53$^{R172H/+}$; Pdx1-Cre (KPC) showed that P2RY2 protein expression was elevated in PanINs and PDAC tissues compared with normal acini (Supplementary Fig. S1B). We further performed IHC staining on tissues from 264 patients with PDAC (named as Renji cohort). P2RY2 expression was significantly higher in PDAC tissues than that in the adjacent tissues (Fig. 1C), and Kaplan–Meier analysis revealed that high expression of the P2RY2 in cancer tissues was associated with a poor prognosis in the patients with PDAC (Fig. 1D). In addition, univariate Cox regression analyses showed that age, TNM stage, tumor size, P2RY2 expression, lymph node metastasis, distant metastasis, and histologic differentiation were significantly associated with overall survival. Meanwhile, a multivariate Cox regression analysis identified that P2RY2 expression, tumor size, T classification, TNM stage, lymph node metastasis, and histologic differentiation as independent predictors of the overall survival in patients with PDAC (Fig. 1E).

P2RY2 activated by extracellular ATP promotes PDAC growth

Because ATP is one of the major natural ligand of P2RY2 (16), we measured the concentration of extracellular ATP (eATP) in the PDAC microenvironment. Human and mouse PDAC tissues were analyzed by measuring the ATP concentration in the tumor interstitial fluid. Consistent with previous studies, eATP levels were higher in tumor tissues than the corresponding adjacent nontumor tissues both in human and mice (Fig. 2A), which led us to hypothesize that P2RY2 activated by eATP in the tumor microenvironment may promote pancreatic cancer growth. To test this hypothesis, the PDAC cell lines AsPC-1 and BxPC-3, with relatively high levels of P2RY2 (Fig. 2B and C), were treated with ATP, UTP, and two other P2RY2 agonists, ATγP and diquafosol (DIQ; ref. 17). As a result, growth of pancreatic cancer cell was significantly enhanced by ATP, UTP, ATγP, and DIQ, but not ADP nor UDP (Fig. 2D). Considering hydrolysis of ATP by ectonucleotidases in tumor cells, prolonged P2RY2 activation (i.e., >24 hours) was performed by addition of ATγP as an activator. As expected, inhibition of P2RY2 with a selective antagonist AR-C118925XX (AR-C; ref. 18) blocked the promoting effect of ATγP on PDAC cells (Fig. 2E). The silenced P2RY2 with short hairpin RNA (shRNA) almost completely abolished the promoting effect

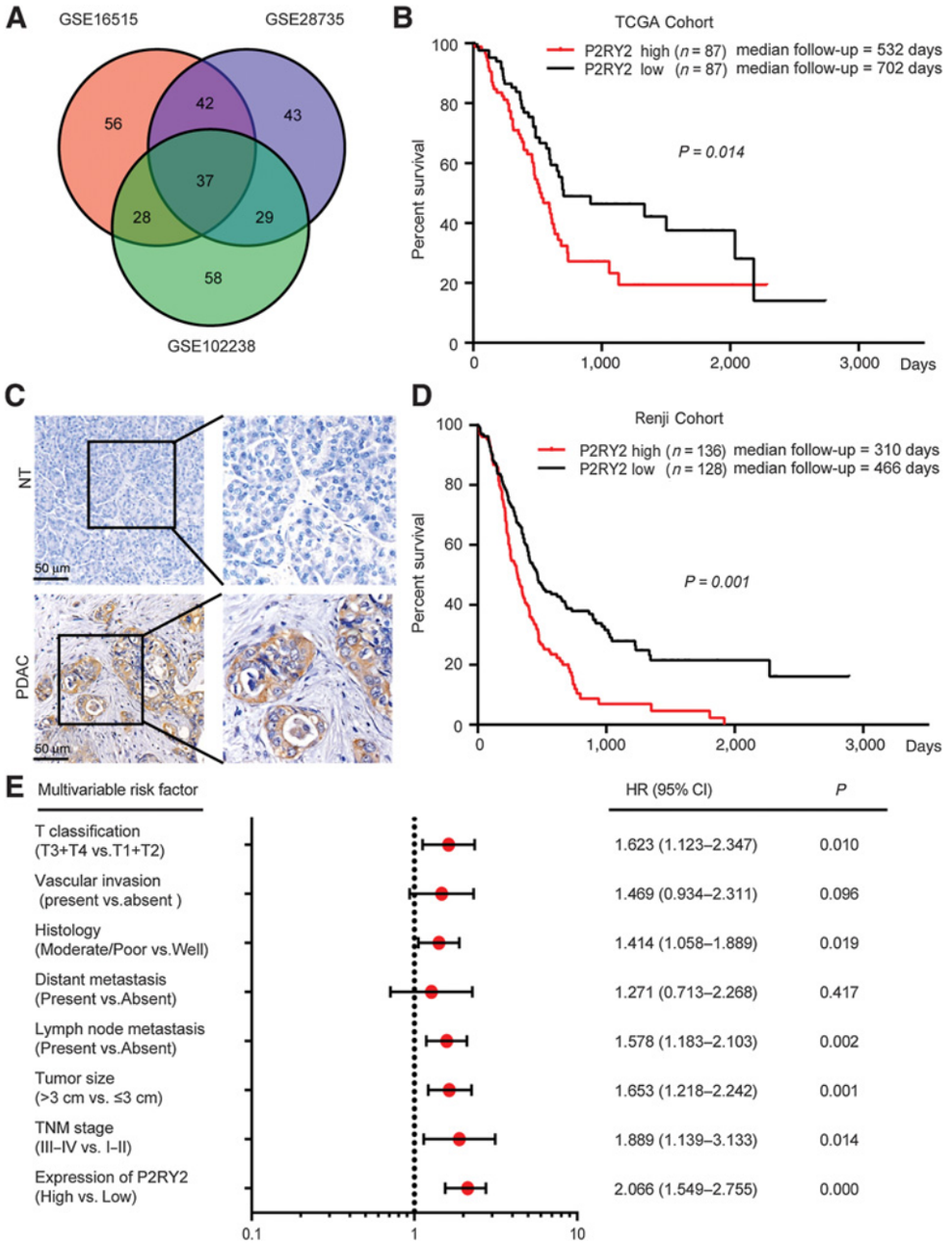

Figure 1.

High P2RY2 expression correlates with poor prognosis in patients with PDAC. **A,** Upregulated expression of GPCRs in PDAC tissue compared with paired nontumor tissues in the GSE16515, GSE28735, and GSE102238 datasets. **B,** Survival curves for patients with PDAC based on the expression of P2RY2 from TCGA data. **C,** IHC staining for P2RY2 in the Renji cohort. NT, nontumor tissues. Scale bar, 50 μm. **D,** Kaplan–Meier analyses of the prognostic value of P2RY2 based on Renji cohort expression data. **E,** Multivariate Cox regression analysis of clinicopathologic factors for overall survival applied in the Renji cohort. CI, confidence interval.

of ATγP on PDAC cells. In addition, restoring P2RY2 by overexpressing shRNA-targeting sequences synonymous mutated P2RY2 in shP2RY2 PDAC cells rescued the cell growth and the ability of colony formation (Fig. 2F and G; Supplementary Fig. S2). Taken together, these data indicate that P2RY2 activated by eATP promotes pancreatic cancer growth.

Activation of P2RY2 promotes cancer cell growth by enhancing glycolysis

To gain comprehensive insight into the mechanism by which activated P2RY2 promotes pancreatic cancer cell growth, the global gene expression in the P2RY2-silenced PDAC cells as compared with control cells after ATP treatment was first

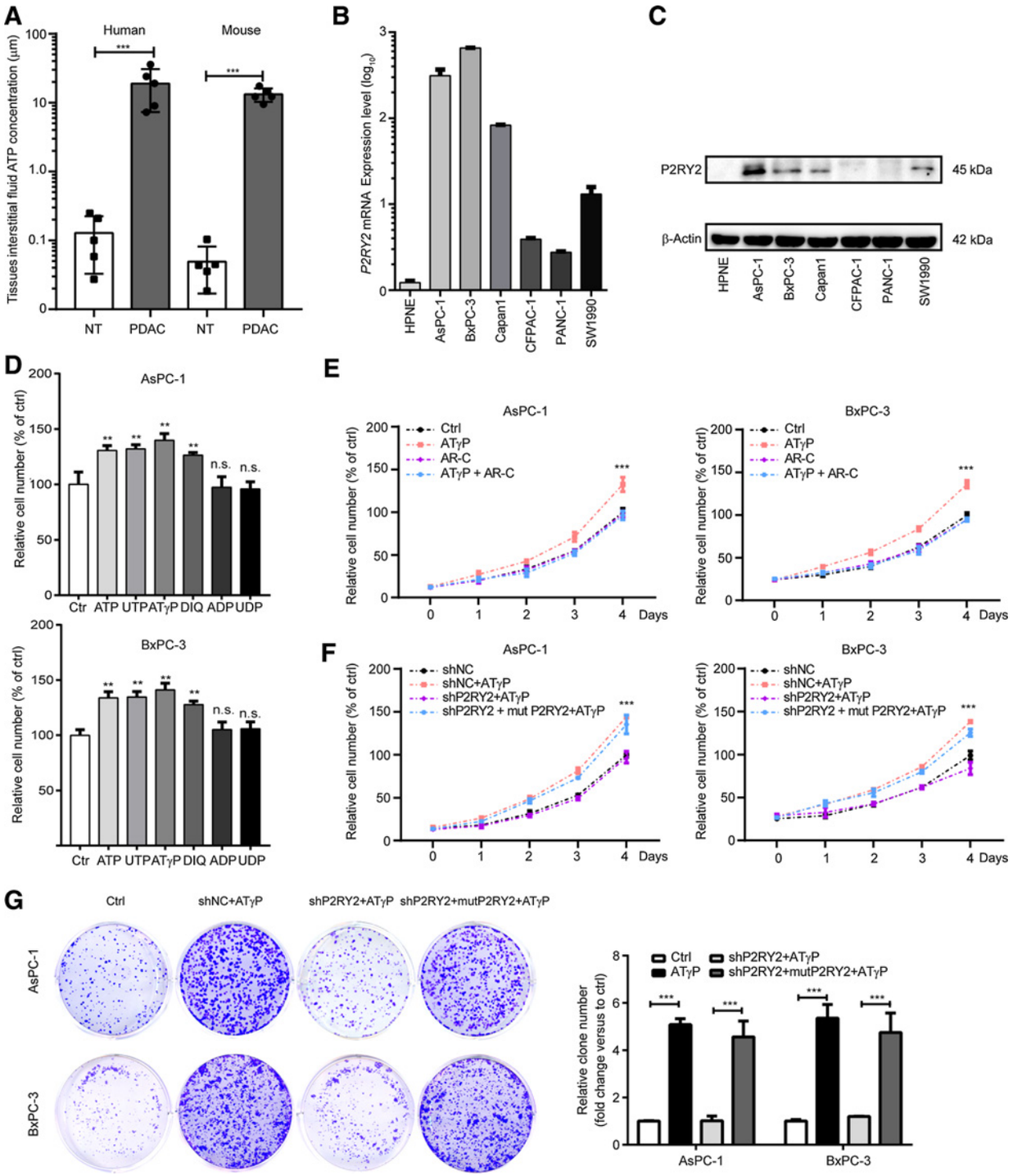

Figure 2.

P2RY2 activation promotes the PDAC cells' growth. **A,** Relative tumor interstitial fluid ATP concentration in PDAC tumor tissues and paired adjacent nontumor tissues (NT) in humans and mice ($n = 5$). **B** and **C,** Relative mRNA and protein expression of P2RY2 in 6 PDAC cell lines and HPNE cell. **D,** Relative cell viability of AsPC-1 and BxPC-3 cells treated with 20 μmol/L ATP, 20 μmol/L UTP, 20 μmol/L ATγP, 10 μmol/L DIQ, 20 μmol/L ADP, and 20 μmol/L UDP for 24 hours, respectively (statistical results vs. the Ctrl group). **E,** Relative cell viability of AsPC-1 and BxPC-3 cells treated with 20 μmol/L ATP, 2 μmol/L AR-C, 20 μmol/L ATγP combined with 2 μmol/L AR-C, respectively. **F,** Relative cell viability of AsPC-1 and BxPC-3 cells stably expressing shNC, shP2RY2, or restored P2RY2 in the presence of 20 μmol/L ATγP or not. **G,** Colony formation assays using AsPC-1 and BxPC-3 cells stably expressing shNC, shP2RY2 or restored P2RY2 in the presence of 20 μmol/L ATγP or not. Representative results of three independent experiments are presented. n.s. = $P > 0.05$; *, $P < 0.05$; **, $P < 0.01$; ***, $P < 0.001$ (two-tailed Student t test for Fig. 2**A**, **D**, and **G**; ANOVA for Fig. 2**E** and **F**).

profiled and analyzed by gene set enrichment analysis (GSEA). The results indicated that genes differentially expressed mostly related to metabolic processes, including genes associated with glycolysis, PI3K–AKT–mTOR signaling, and c-Myc targets, suggesting that activation of the P2RY2 may alter the glycolytic flux in PDAC cells (Fig. 3A). Several key genes in the glycolysis pathway including *GLUT1*, *HK2*, *PFKFB3*, *PGAM1*, and *LDHA* were significantly downregulated in the P2RY2-silenced PDAC cells compared with control cells in the presence of ATP (Fig. 3B; Supplementary Fig. S3A). Alteration of *GLUT1*, *HK2*, *PFKFB3*, *PGAM1*, and *LDHA* were further confirmed by real-time qPCR (Fig. 3C). To gain further investigation into the effects of the eATP on PDAC cells, a glycolysis stress test using ECAR was performed to measure the glycolytic activity in the PDAC cells. As compared with the control, the PDAC cells treated with ATP showed a significant increment in the glycolytic capacity and the glycolytic reserve. This effect was reversed by the silenced P2RY2 (Fig. 3D). However, eATP and P2RY2 inhibition had no significant effect on the OCR of PDAC (Fig. 3E; Supplementary Fig. S3B). The proliferative effect of ATP on the PDAC cells was abolished by either glucose in the medium was replaced by galactose or the cells treated with a glycolytic inhibitor 2-deoxy-d-glucose (2-DG; Fig. 3F and G). Taken together, these data suggest that the tumorigenic effect by activation of the P2RY2 may largely result from its enhancement of glycolysis.

P2RY2 enhances PDAC glycolysis by activating the PI3K/AKT–mTOR pathway

To further understand the molecular mechanism underlying regulation of P2RY2 on glycolysis, two crucial transcriptional factors c-Myc and HIF1α, which are key regulators in glycolysis, were measured upon ATP treatment in the PDAC cells. The results showed that the expression levels of both c-Myc and HIF1α were significantly upregulated in P2RY2-activated cells than those in control cells (Fig. 4A). Knockdown of both c-Myc and HIF1α impaired the glycolytic activity upon ATP induction (Supplementary Fig. S4). To understand an association of the P2RY2 to these two transcription factors, the intermediate signaling components MAPK/ERK and PI3K/AKT, the canonical downstream pathways of P2RY2 were examined. As ERK antagonist U0126 did not significantly compromise the ATP-enhanced glycolysis (Supplementary Fig. S5), further study on the PI3K/AKT pathway was undertaken. Our study showed that activation of the P2RY2 led to significant enhancement of AKT signaling including its downstream targets, mTOR and P70S6K (Fig. 4A), suggesting that c-Myc and HIF1α may be upregulated by ATP-P2RY2 through activation of the PI3K/AKT signaling pathway. These results obtained above were further confirmed by using inhibitors of P2RY2 receptors, PI3K and mTOR. As expected, the activation of PI3K/AKT–mTOR pathway and the upregulation of c-Myc and HIF1α were largely abolished after treatment with these inhibitors (Fig. 4A). Similarly, knockdown P2RY2 with shRNA also repressed the PI3K/AKT–mTOR signaling and replenishing P2RY2 expression in PDAC cells resulting in the restoration of their sensitivity to extracellular ATP stimulation (Supplementary Fig. S5). Consistently, the effects of ATP on glycolytic enzyme expression (Fig. 4B), ECAR (Fig. 4C), glucose consumption (Fig. 4D), and lactate production (Fig. 4E), were completely abolished by the P2RY2 antagonist, LY294002 or rapamycin, respectively. Taken together, these findings indicate that ATP-P2RY2 activates PI3K/AKT–mTOR signaling, elevates the expression of HIF1α and c-Myc, and ultimately enhances PDAC cell glycolysis.

P2RY2 activates the PI3K/AKT pathway by crosstalk with PDGFR

We next investigated the mechanism of how P2RY2 activated PI3K/AKT–mTOR pathway. Previous works reported that P2RY2 could activate PI3K/AKT signaling by crosstalk with EGFR or PDGFR (19). However, PDAC cell lines treated with ATP did not show any obvious EGFR activation (Fig. 5A). As GESA analysis showed that PDGF_UP V1_ UP enriched in AsPC-1 under the treatment of ATP (Supplementary Fig. S7A), we next detect whether PDGFRβ, the dominant expressed PDGFR subtype (Supplementary Fig. S7B), was activated by ATP treatment in PDAC cells. Immunoblot results showed that phosphorylated PDGFRβ level increased in a time-dependent manner after treatment with ATP (Fig. 5A). In addition, CP673451, a selective PDGFR receptor antagonist, could prevent ATP-induced glycolysis enhancement but not the EGFR inhibitor AG1478 (Fig. 5B). Furthermore, we tried to figure out the intermediator between P2RY2 and PDGFRβ. Src family kinases (SFK) are reported as a kinase mediated the crosstalk between GPCRs and RTKs (19, 20). The SFK expression in TCGA-PAAD dataset was analyzed. The results showed that Src, Lyn, and Yes1 were the dominantly expressed SFK members in PDAC (Supplementary Fig. S8). After silencing with siRNA, respectively, in PDAC cells, only siYes1 greatly impaired ATP-enhanced glycolysis (Fig. 5C), indicating that Yes1 may be the link for the crosstalk between P2RY2 and PDGFRβ. In addition, endogenous immunoprecipitation assays showed that p-Yes1 and p-PDGFRβ interaction was strengthened in the ATP treatment (Fig. 5D). Furthermore, Yes1 was detected in the antiphosphorylated PDGFRβ precipitates (Fig. 5D). Consistently, the interaction between Yes1 and PDGFRβ was further confirmed by an immunofluorescence staining method. The results showed that both Yes1 and PDGFRβ were colocalized in human and mouse PDAC tumor tissues (Fig. 5E). To further investigate whether Yes1 serves as an intermediary signaling molecule between P2RY2 and PDGFRβ-PI3K/AKT, Yes1 was silenced by siRNA in the PDAC cells. As expected, knockdown of Yes1 greatly diminished the ATP-induced activation of PDGFRβ, PI3K/AKT–mTOR and reduced the expression of both c-Myc and HIF1α (Fig. 5F). Furthermore, activated P2RY2-mediated glycolysis was also inhibited by Yes1 silencing, as determined by expression levels of the glycolytic enzymes (Fig. 5G), glucose consumption (Fig. 5H), and lactate production (Fig. 5I). Together, these data suggest that Yes1 mediates the crosstalk between P2RY2 and PDGFRβ, which subsequently triggers PI3K/AKT signaling.

Genetic or pharmacologic inhibition of P2RY2 suppresses PDAC cell growth *in vivo*

To investigate the *in vivo* function of the P2RY2, subcutaneous, orthotopic mouse models and an inflammation-driven PDAC model were generated. First, human PDAC cells expressing either scramble or P2RY2 shRNA were inoculated subcutaneously in mice (termed as either shNC mice or shP2RY2 mice, respectively). The results showed that shNC mice developed larger tumors in size than shP2RY2 mice (Supplementary Fig. S8A and S8B). Similarly, blocking the P2RY2 with AR-C

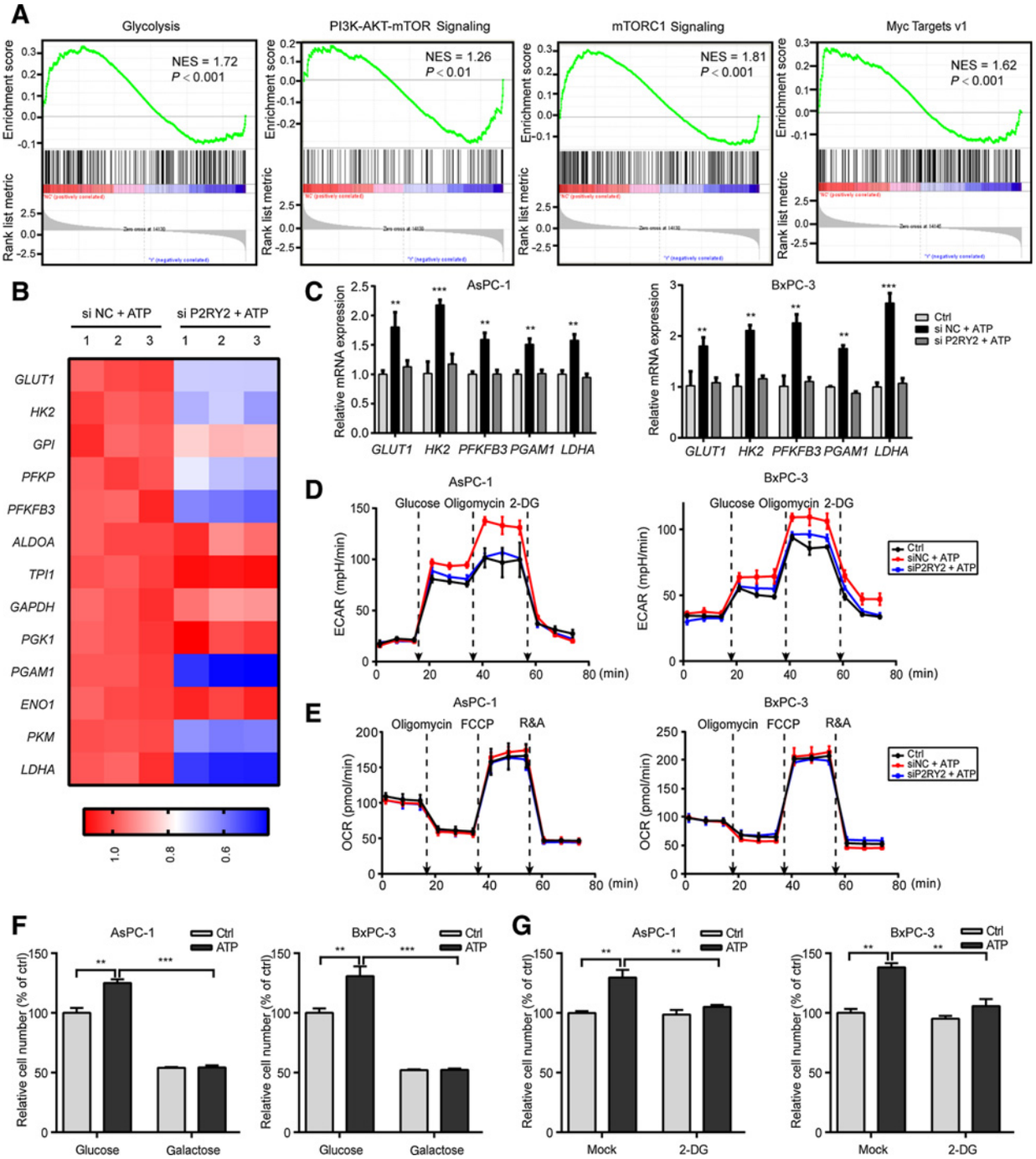

Figure 3.

P2RY2 activation enhances PDAC cell glycolysis. **A,** Gene set enrichment analysis (GSEA) using hallmark gene sets was performed to compare the AsPC-1 siNC group and siP2RY2 group treated with ATP for 24 hours. NES, normalized enrichment score. **B,** A heatmap showing the expression of the glycolysis-related genes across AsPC-1 NC samples and P2RY2 knockdown with siRNA samples in the presence of ATP. **C,** Relative mRNA levels of glycolysis-related genes of PDAC with P2RY2 inhibited by siRNA or not in the presence ATP treatment for 24 hours. **D,** Glycolytic function of PDAC cell lines versus ATP treatment for 24 hours and P2RY2 knockdown by siRNA plus ATP treatment for 24 hours as measured by the ECAR ($n = 3$). **E,** Mitochondrial stress test of PDAC cell lines versus ATP treatment for 24 hours and P2RY2 knockdown by siRNA plus ATP treatment for 24 hours as measured by the OCR ($n = 3$). R&A, rotenone and antimycin A. **F,** PDAC relative cell viability after treatment with Ctrl or ATP in normal (with glucose) or galactose medium for 24 hours ($n = 5$). **G,** PDAC relative cell viability after treatment with Ctrl, ATP (20 μmol/L), 2-DG (5 mmol/L) or ATP (20 μmol/L) + 2-DG (5 mmol/L) for 24 hours ($n = 5$). Data are represented as the mean ± SD (two-tailed Student *t* test for **C, F**, and **G**).

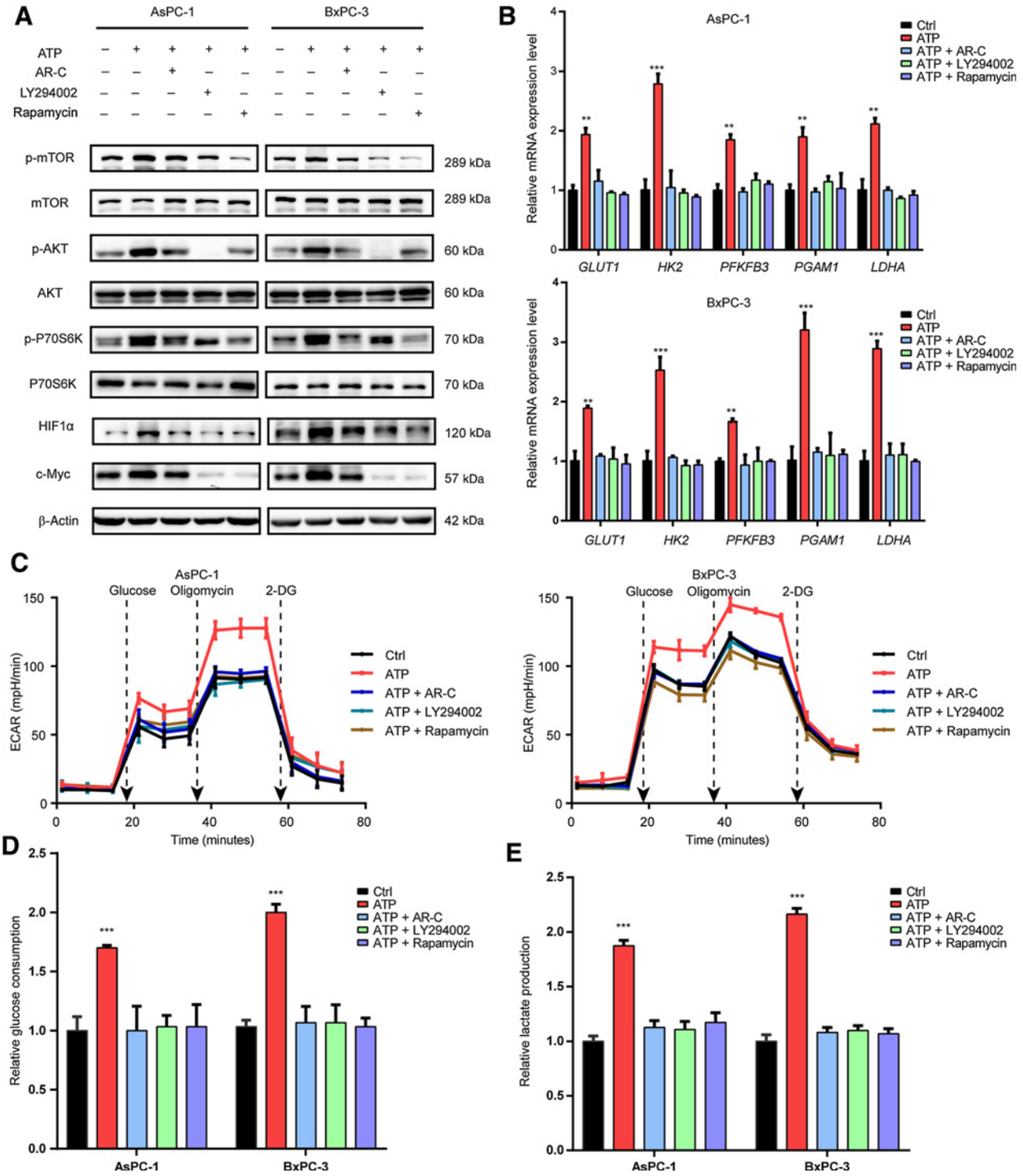

Figure 4.

P2RY2 activation triggers the PI3K/AKT–mTOR pathway and elevates c-Myc and HIF1α expression. **A,** Western blot analysis of phospho-mTOR (p-mTOR), mTOR, phospho-AKT(p-AKT), AKT, phospho-P70S6K (p-P70S6K), P70S6K, c-Myc, and HIF1α expression in lysates derived from PDAC cells treated with ATP or ATP combined with AR-C(2 μmol/L), LY294002(20 μmol/L), or rapamycin(50 nmol/L), respectively, for 24 hours. **B,** Relative mRNA levels of glycolysis-related genes in the presence of ATP or ATP combined with AR-C, LY294002, or rapamycin, respectively, for 24 hours. **C,** Glycolytic function of PDAC cell lines under the indicated treatments as measured by extracellular acidification rate (ECAR, $n = 3$). **D,** Glucose consumption of PDAC cell lines under the indicated treatments ($n = 3$). **E,** Lactate production of PDAC cell lines under the indicated treatments ($n = 3$; *, $P < 0.05$; **, $P < 0.01$; ***, $P < 0.001$; ANOVA test for **B**, **D**, and **E**).

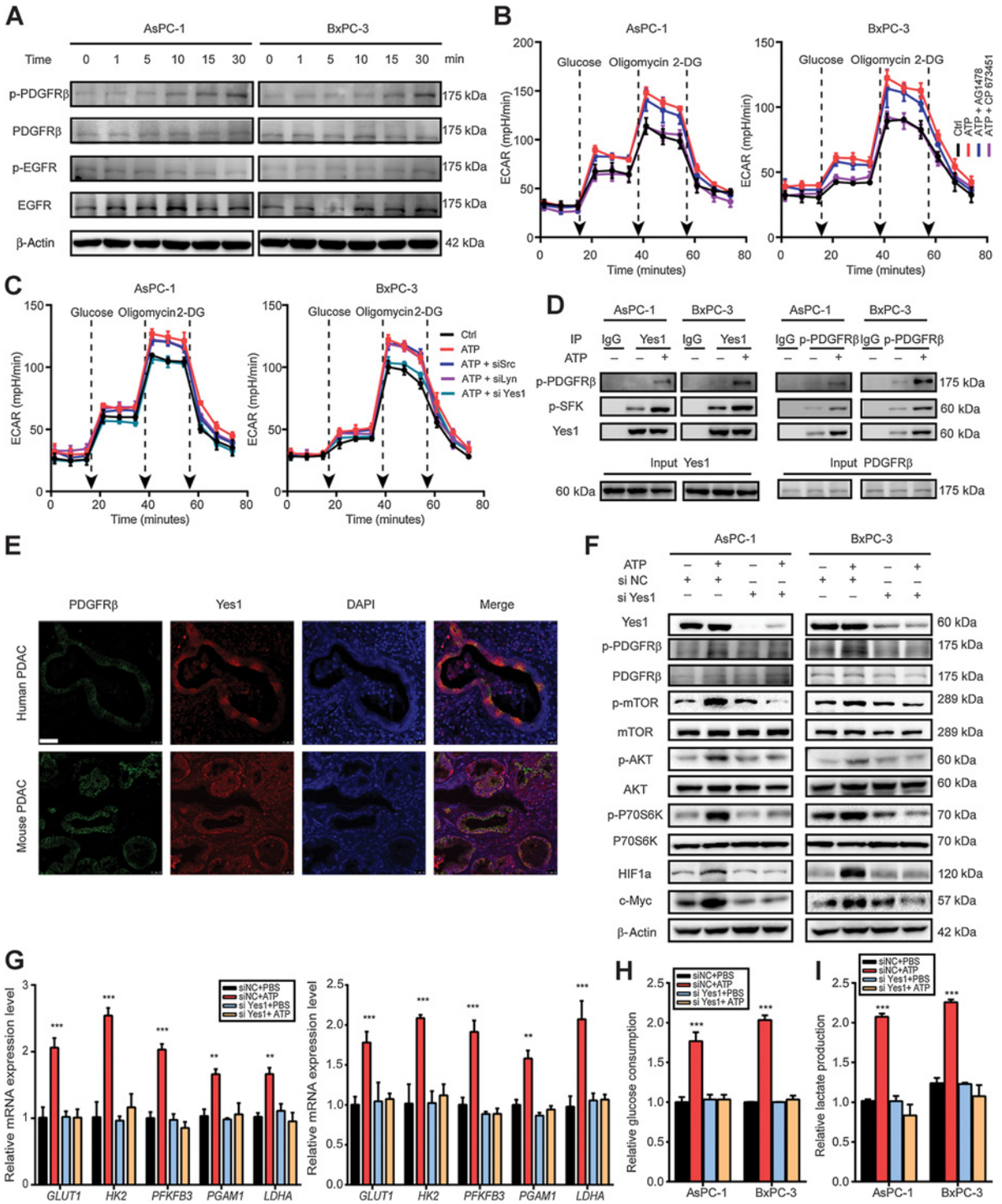

Figure 5.

P2RY2 activates PI3K-AKT pathway by crosstalk with PDGFR. **A,** Immunoblots of p-PDGFRβ, PDGFRβ, p-EGFR, EGFR in AsPC-1 and BxPC-3 cells treated with 20 μmol/L ATP for different time points. **B,** Glycolytic function of PDAC cell lines treated with ATP or ATP plus CP673451 (10 nmol/L), AG1478 (10 nmol/L) as measured by ECAR for 24 hours. **C,** Glycolytic function of PDAC cell lines treated with ATP or ATP plus Src, Lyn, and Yes1 silenced by siRNA, respectively, as measured by ECAR. **D,** Co-immunoprecipitation of Yes1 and p-PDGFRβ in PDAC cell lines treated with ATP for 24 hours or not. **E,** Immunofluorescence of Yes1 and p-PDGFRβ in human and mouse PDAC tissues. Scale bar, 50 μm. **F,** Immunoblot analysis of PDAC cells that Yes1 knockdown by siRNA or Ctrl in the presence or absence of ATP stimulation. **G–I,** The relative mRNA levels of glycolytic genes (**G**, $n = 3$), ECAR (**H**, $n = 3$), glucose consumption, and lactate production (**I**, $n = 3$) in si-Ctrl and si-Yes1 cells were measured in the presence or absence of ATP stimulation (*, $P < 0.05$; **, $P < 0.01$; ***, $P < 0.001$).

reduced tumor burden in the subcutaneous model (Fig. 6A). In addition, the immunoreactivity of the proliferation index proliferating cell nuclear antigen (PCNA) was significantly reduced both in shP2RY2 and AR-C–treated xenograft tissues compared with corresponding controls (Supplementary Fig. S8C). Second, the orthotopic PDAC model was established by orthotopically transplanting luciferase-expressing Panc02 cells (a mouse PDAC cell line). Orthotopic tumor growth was monitored by bioluminescence imaging and expressed as luminescence intensity (Fig. 6B). The bioluminescence data revealed that AR-C–treated mice showed slower rate of tumor growth than the control mice (Fig. 6C). With regard to the synergistic effects for first-line therapy, both AR-C (10 mg/kg) and gemcitabine (50 mg/kg) were administered every 5 days to implanted mice, which resulted in smaller tumors and extended overall survival compared with the AR-C or gemcitabine treatment alone (Fig. 6D). Orthotopic tumors were resected, and histologic sections were investigated. As expected, a significant inhibition in tumor growth, PDGFRβ and PI3K/AKT–mTOR signaling in mice treated with AR-C was observed (Fig. 6E). Furthermore, the inflammation-driven PDAC model, KC mice treated with cerulein, was used to assay targeting P2RY2 effect in PDAC at early stage. AR-C–treated KC mice presented with more normal acinar tissue and less PanIN area in comparison with control mice (Fig. 6F and G). Collectively, targeting P2RY2 inhibits PDAC progression *in vivo* and that the combination of AR-C and gemcitabine may provide an additional treatment benefit.

Discussion

Accumulating evidence has shown that the tumor microenvironment greatly supports cancer progression by facilitating cancer cell growth, reprogramming metabolism, and inhibiting the immune response (21–23). Thus, we hypothesized that removing the support from the tumor microenvironment would halt cancer progression. Recently, extracellular energetics in the tumor microenvironment, especially ATP, has attracted the attention of researchers; however, their roles and mechanism in PDAC maintenance and progression remain largely unknown. This study demonstrated that P2RY2 expression was upregulated and predicted poor prognosis in PDAC. Through functional and mechanistic studies, we identified activated P2RY2 as a metabolism regulator by crosstalk with PDGFRβ, which activated the PI3K/AKT/mTOR pathway and then elevated c-Myc and HIF1α expression, ultimately resulting in enhanced glycolysis. Targeting P2RY2 greatly repressed pancreatic cancer growth by blocking metabolic reprogramming in the eATP-induced cancer cells (Fig. 6H).

Previous studies have reported that extracellular ATP promotes cancer progression by supporting tumor cell growth and enhancing metastasis. It has been demonstrated that extracellular ATP induces intracellular Ca^{2+} increases and promotes cancer cell growth through activation of purinergic receptors (24). ATP derived from platelet activates P2RY2 on the membrane of endothelial cells, leading to opening of the endothelial barrier and tumor cell migration through the endothelial layer (25). In addition, phosphocreatinine released into the extracellular space by liver cells encountering hepatic hypoxia is imported through the SLC6A8 transporter to accelerate colon cancer cell energy production (26). Our data support the concept that extracellular energetics promote cancer progression. Our results, for the first time, showed that eATP promoted pancreatic cancer progression by reprogramming cancer cell metabolism. Transcriptomic and metabolic analyses revealed that the growth-promoting roles of ATP were largely dependent on glycolysis. Furthermore, the mechanism of metabolic conversion induced by ATP relied on increased c-Myc and HIF1α expression. It has been reported that other factors could also regulate c-Myc and HIF1α expression in PDAC, such as TGFβ (27) and APE1 (28). Because of the heterogeneity and complexity of PDAC, many intercellular and extracellular factors could affect the status of c-Myc and HIF1α under different conditions or tumor progression stages. Consistent with our results, previous studies in breast cancer and 293T cells also showed that P2RY2 could regulate c-Myc and HIF1α expression (29, 30), indicating that c-Myc and HIF1α regulated by P2RY2 might be a relative common mechanism in the presence of extracellular ATP.

P2RY2, a Gq-coupled GPCR, has been reported to be involved in HIV infection (31) and to promote immune cell infiltration (32, 33). Previous studies have shown that P2RY2 is widely expressed in cancers, and its prosurvival roles have been well summarized by Burnstock and colleagues (34) and Virgilio and colleagues (35). However, the roles and involved mechanisms of P2RY2 in PDAC progression remain poorly understood. P2RY2 has been reported to activate the MEK–ERK (36, 37) and PI3K–AKT pathways (38–40). Our data showed that PI3K–AKT was involved in P2RY2 activation–induced metabolism reprogramming, but not MEK–ERK signaling. The crosstalk between GPCRs and RTKs was widely reported, which was mainly mediated by the Src family members (SFKs). Preceding works showed that P2RY2 can trigger EGFR and PDGFR signaling after activation by nature agonists (19). In breast cancer, P2RY2 can activate EGFR through Src (36). In our study, we found that P2RY2 can establish crosstalk with PDGFR mediated by Yes1, which directly interacts with PDGFR. As for how ATP-mediated P2RY2 activation promotes activation of Yes1, there are several potential mechanisms. First, P2RY2 could directly interact with Yes1. The third intracellular loop and C-terminus of GPCR have proline-rich motifs, which could serve as docking sites for SFKs SH3 domain (19). Second, SFKs could be regulated by heterotrimeric G proteins. Several works indicated that direct interactions between SFKs and Gα subunits regulate SFKs activity. The switch II region of the Ga subunit could bind on the catalytic domains of SFKs, which indirectly disrupts the intramolecular associations of SFKs, resulting in SFKs activation (41). Third, SFKs could be activated by GPCR through the scaffolds known as β-arrestins. β-arrestins work as signal transducers, which could bind directly to SFKs and recruit it to agonist-occupied GPCRs (42). However, the specific mechanism of P2RY2 activation, Yes1, in PDAC remains to be determined and needs more efforts.

In normal physiologic conditions, extracellular concentrations of ATP are low and tightly modulated by ectonucleotidases (CD39 and CD73). However, extracellular ATP concentrations can be sharply elevated under situations of stress, such as hypoxia, nutrient deprivation, low pH, or inflammation (43). Therefore, it is not surprising that increased ATP concentrations in the tumor microenvironment have been widely reported (44). Consistent with previous studies, we demonstrated that the ATP concentration was elevated in

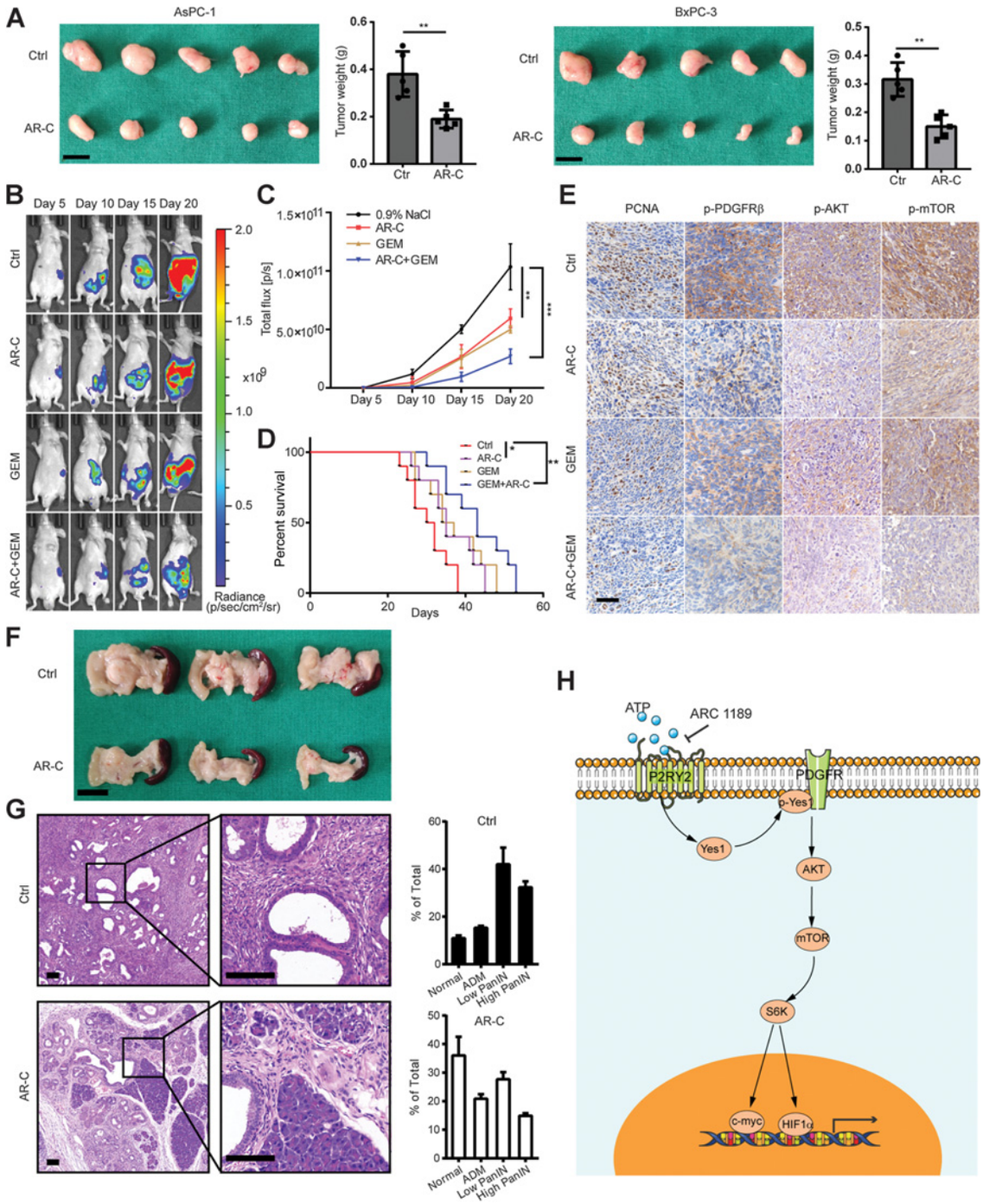

Figure 6.

Targeting P2RY2 suppresses tumor growth *in vivo*. **A,** Subcutaneous xenografts transplanted with AsPC-1 and BxPC-3 cells treated with or without AR-C ($n = 5$). Scale bar, 1 cm. **B,** Representative bioluminescence photograph of mice orthotopically implanted with luciferase-expressing Panc02 cells respectively treated with 0.9% NaCl, AR-C (10 mg/kg) or gemcitabine (50 mg/kg) alone or treated with combination of AR-C and gemcitabine every 5 days. **C,** Quantification of the total flux luminescence of the mice as measured by IVIS at different time points ($n = 5$). **D,** Kaplan–Meier survival curve of mice implanted with Panc02 cells treated with 0.9% NaCl, AR-C, gemcitabine or the combination of AR-C and gemcitabine ($n = 10$). **E,** Representative IHC images of PCNA, p-PDGFRβ, p-Akt, p-mTOR from orthotopic PDAC mice under indicated treatment. Scale bar, 50 μm. **F,** Pancreas of ceruletide-injected KC mice subjected to AR-C or Ctrl treatment. Scale bar, 1 cm. **G,** Representative images of H&E staining of ceruletide-injected KC mice at 20 weeks on subjected to AR-C or Ctrl treatment and pathologic analysis of pancreas depicted ($n = 3$). Scale bar, 100 μm. **H,** Proposed model for extracellular ATP promotes the growth of PDAC cells (n.s. = $P > 0.05$; *, $P < 0.05$; **, $P < 0.01$; ***, $P < 0.001$; two-tailed Student *t* test for **A**; ANOVA test for **C**; and log-rank Mantel–Cox test for **D**).

the PDAC tumor microenvironment according to the interstitial fluid isolation method as reported by Eil and colleagues (14) We realize that the method we used to measure ATP cannot detect the ATP concentration in real-time as reported by Francesco and colleagues (45). Moreover, the roles of extracellular ATP in cancer remain controversial. ATP has been reported to have suppressive or promoting effects on cancer growth by different research groups (46, 47). However, it is clear that the suppressive or promoting effect of extracellular ATP on cancer growth is largely dependent on the receptor subtype. P2Y1R and P2Y2R have a promoting role on cancer growth, while P2 × 7R mainly plays a suppressive role. Another explanation for the controversial roles of ATP in the tumor microenvironment might be caused by the different effects of ATP with its breakdown products on immune response regulation. Indeed, it has been demonstrated that ATP is recognized by immune cells (48). Thus, while analyzing P2RY2 inhibition in inflammation-driven PDAC model, we cannot completely rule out the possibility that altered immune responses with AR-C treatment contributed to the tumor-suppressive effects.

In conclusion, our results demonstrate that the increased ATP in the PDAC microenvironment binds to the P2RY2 receptor, which triggers PDGFR signaling mediated by Yes1. This crosstalk subsequently activates the PI3K–AKT–mTOR pathway and increases the expression of both c-Myc and HIF1α and eventually leads to an enhanced glycolysis in PDAC cells. Furthermore, targeting P2RY2 significantly inhibits PDAC progression. Taken together, our results provide new insight into how extracellular ATP affects PDAC progression and suggest that targeting P2RY2 might constitute a new approach for PDAC treatment.

Disclosure of Potential Conflicts of Interest

No potential conflicts of interest were disclosed.

Authors' Contributions

Conception and design: L.-P. Hu, S.-H. Jiang, G.G. Xiao, Z.-G. Zhang
Development of methodology: L.-P. Hu, Q. Li, L.-L. Zhu
Acquisition of data (provided animals, acquired and managed patients, provided facilities, etc.): L.-P. Hu, S.-H. Jiang, L.-Y. Tao, Q. Li, L.-L. Zhu, M.-W. Yang, Y.-S. Jiang, Y.-L. Zhang, J. Li, Y.-W. Sun
Analysis and interpretation of data (e.g., statistical analysis, biostatistics, computational analysis): L.-P. Hu, S.-H. Jiang, G.-A. Tian, Q. Yang, Z.-G. Zhang
Writing, review, and/or revision of the manuscript: L.-P. Hu, S.-H. Jiang, G.-A. Tian, Y.-L. Zhang, Q. Yang, G.G. Xiao, Z.-G. Zhang
Administrative, technical, or material support (i.e., reporting or organizing data, constructing databases): X.-X. Zhang, S.-H. Jiang, L.-Y. Tao, Y.-M. Huo, Y.-S. Jiang, X.-Y. Cao, X.-M. Yang, Y.-H. Wang, J. Li, Y.-W. Sun
Study supervision: S.-H. Jiang, G.G. Xiao, Z.-G. Zhang

Acknowledgments

This study was supported by the National Natural Science Foundation of China (81672358, to Z.-G. Zhang; 81871923, to J. Li; 81872242, to Y.-L. Zhang), the Shanghai Municipal Education Commission—Gaofeng Clinical Medicine Grant Support (20181708, to Z.-G. Zhang), the Natural Science Foundation of Shanghai (17ZR1428300, to J. Li), and Shanghai Municipal Health Bureau (2018BR32, to Z.-G. Zhang). We thank Prof. Jing Xue for the kindly gift Panc 02 mouse PDAC cell line and Ruizhe He for tumor interstitial fluid collection. We thank Dr. Xueli Zhang for critical reading of this manuscript.

The costs of publication of this article were defrayed in part by the payment of page charges. This article must therefore be hereby marked *advertisement* in accordance with 18 U.S.C. Section 1734 solely to indicate this fact.

Received July 17, 2018; revised October 15, 2018; accepted November 2, 2018; published first November 12, 2018.

References

1. Siegel RL, Miller KD, Jemal A. Cancer statistics, 2018. CA Cancer J Clin 2018;68:7–30.
2. Makohonmoore A, Iacobuziodonahue CA. Pancreatic cancer biology and genetics from an evolutionary perspective. Nat Rev Cancer 2016;16:553–65.
3. Rahib L, Smith BD, Aizenberg R, Rosenzweig AB, Fleshman JM, Matrisian LM. Projecting cancer incidence and deaths to 2030: the unexpected burden of thyroid, liver, and pancreas cancers in the United States. Cancer Res 2014;74:2913–21.
4. Liotta LA, Kohn EC. The microenvironment of the tumour–host interface. Nature 2001;411:375–9.
5. Bergmann U, Funatomi H, Yokoyama M, Beger HG, Korc M. Insulin-like growth factor I overexpression in human pancreatic cancer: evidence for autocrine and paracrine roles. Cancer Res 1995;55:2007–11.
6. Zhang Y, Zoltan M, Riquelme E, Xu H, Sahin I, Castro-Pando S, et al. Immune cell production of interleukin 17 induces stem cell features of pancreatic intraepithelial neoplasia cells. Gastroenterology 2018;155:210–23.
7. Rubie C, Frick VO, Ghadjar P, Wagner M, Grimm H, Vicinus B, et al. CCL20/CCR6 expression profile in pancreatic cancer. J Transl Med 2010;8:45-.
8. Sousa CM, Biancur DE, Wang X, Halbrook CJ, Sherman MH, Zhang L, et al. Pancreatic stellate cells support tumour metabolism through autophagic alanine secretion. Nature 2016;536:479–83.
9. Lefkowitz RJ. Historical review: a brief history and personal retrospective of seven-transmembrane receptors. Trends Pharmacol Sci 2004;25:413–22.
10. Dorsam RT, Gutkind JS. G-protein-coupled receptors and cancer. Nat Rev Cancer 2007;7:79.
11. Hayakawa Y, Sakitani K, Konishi M, Asfaha S, Niikura R, Tomita H, et al. Nerve growth factor promotes gastric tumorigenesis through aberrant cholinergic signaling. Cancer Cell 2017;31:21–34.
12. Hutchings CJ, Koglin M, Olson WC, Marshall FH. Opportunities for therapeutic antibodies directed at G-protein-coupled receptors. Nat Rev Drug Discov 2017;16:787.
13. Hauser AS, Chavali S, Masuho I, Jahn LJ, Martemyanov KA, Gloriam DE, et al. Pharmacogenomics of GPCR drug targets. Cell 2018;172:41–54.e19.
14. Eil R, Vodnala SK, Clever D, Klebanoff CA, Sukumar M, Pan JH, et al. Ionic immune suppression within the tumour microenvironment limits T cell effector function. Nature 2016;537:539–43.
15. Renz BW, Takahashi R, Tanaka T, Macchini M, Hayakawa Y, Dantes Z, et al. beta2 Adrenergic-neurotrophin feedforward loop promotes pancreatic cancer. Cancer Cell 2018;33:75–90.
16. Ralevic V, Burnstock G. Receptors for purines and pyrimidines. Pharmacol Rev 1998;50:413–92.
17. Lau OCF, Samarawickrama C, Skalicky SE. P2Y2 receptor agonists for the treatment of dry eye disease: a review. Clin Ophthalmol 2014;8:327–34.
18. Rafehi M, Burbiel JC, Attah IY, Abdelrahman A, Muller CE. Synthesis, characterization, and *in vitro* evaluation of the selective P2Y2 receptor antagonist AR-C118925. Purinergic Signal 2017;13:89–103.
19. Liu J, Liao Z, Camden J, Griffin KD, Garrad RC, Santiago-Pérez LI, et al. Src homology 3 binding sites in the P2Y2 nucleotide receptor interact with Src and regulate activities of Src, proline-rich tyrosine kinase 2, and growth factor receptors. J Biol Chem 2004;279:8212–8.
20. Natarajan K, Berk BC. Crosstalk coregulation mechanisms of G protein-coupled receptors and receptor tyrosine kinases. Methods Mol Biol 2006;332:51–77.
21. Whiteside T. The tumor microenvironment and its role in promoting tumor growth. Oncogene 2008;27:5904.

22. Martinez-Outschoorn UE, Peiris-Pagés M, Pestell RG, Sotgia F, Lisanti MP. Cancer metabolism: a therapeutic perspective. Nat Rev Clin Oncol 2017;14:11.
23. Pickup MW, Novitskiy SV, Moses HL. The roles of TGFβ in the tumour microenvironment. Nat Rev Cancer 2013;13:788–99.
24. Xie R, Xu J, Wen G, Jin H, Liu X, Yang Y, et al. The P2Y2 nucleotide receptor mediates the proliferation and migration of human hepatocellular carcinoma cells induced by ATP. J Biol Chem 2014;289: 19137–49.
25. Schumacher D, Strilic B, Sivaraj KK, Wettschureck N, Offermanns S. Platelet-derived nucleotides promote tumor-cell transendothelial migration and metastasis via P2Y2 receptor. Cancer Cell 2013;24:130–7.
26. Loo JM, Scherl A, Nguyen A, Man FY, Weinberg EM, Zeng Z, et al. Extracellular metabolic energetics can promote cancer progression. Cell 2015;160:393–406.
27. Hessmann E, Schneider G, Ellenrieder V, Siveke JT. MYC in pancreatic cancer: novel mechanistic insights and their translation into therapeutic strategies. Oncogene 2016;35:1609–18.
28. Logsdon DP, Grimard M, Shahda S, Zyromski N, Schipani E, Carta F, et al. Regulation of HIF1α under hypoxia by APE1/Ref-1 impacts CA9 expression: Dual targeting in patient-derived 3D pancreatic cancer models. Mol Cancer Ther 2016;15;2722–32.
29. Zhang J, Liu Y, Yang H, Zhang H, Tian X, Fang W. ATP-P2Y2-β-catenin axis promotes cell invasion in breast cancer cells. Cancer Sci 2017; 108:1318–27.
30. Amoroso F, Falzoni S, Adinolfi E, Ferrari D, Virgilio FD. The P2X7 receptor is a key modulator of aerobic glycolysis. Cell Death Dis 2012; 3:e370.
31. Séror C, Melki M-T, Subra F, Raza SQ, Bras M, Saïdi H, et al. Extracellular ATP acts on P2Y2 purinergic receptors to facilitate HIV-1 infection. J Exp Med 2011;208:1823–34.
32. Burnstock G, Boeynaems J-M. Purinergic signalling and immune cells. Purinergic Signal 2014;10:529–64.
33. Idzko M, Ferrari D, Eltzschig HK. Nucleotide signalling during inflammation. Nature 2014;509:310–7.
34. White N, Burnstock G. P2 receptors and cancer. Trends Pharmacol Sci 2006;27:211–7.
35. Di Virgilio F, Adinolfi E. Extracellular purines, purinergic receptors and tumor growth. Oncogene 2017;36:293–303.
36. Martinezramirez AS, Garay E, Garciacarranca A, Vazquezcuevas F. The P2RY2 receptor induces carcinoma cell migration and EMT through cross-talk with epidermal growth factor receptor. J Cell Biochem 2016; 117:1016–26.
37. Bilbao PS, Boland R, Santillán G. ATP modulates transcription factors through P2Y 2 and P2Y 4 receptors via PKC/MAPKs and PKC/Src pathways in MCF-7 cells. Arch Biochem Biophys 2010;494:7–14.
38. Taboubi S, Milanini J, Delamarre E, Parat F, Garrouste F, Pommier G, et al. G alpha(q/11)-coupled P2Y2 nucleotide receptor inhibits human keratinocyte spreading and migration. FASEB J 2007;21:4047–58.
39. Bilbao PS, Santillan G, Boland R. ATP stimulates the proliferation of MCF-7 cells through the PI3K/Akt signaling pathway. Arch Biochem Biophys 2010;499:40–8.
40. Huwiler A, Rolz W, Dorsch S, Ren S, Pfeilschifter J. Extracellular ATP and UTP activate the protein kinase B/Akt cascade via the P2Y2 purinoceptor in renal mesangial cells. Br J Pharmacol 2002;136:520–9.
41. Ma YC, Huang J, Ali S, Lowry W, Huang XY. Src tyrosine kinase is a novel direct effector of G proteins. Cell 2000;102:635–46.
42. Luttrell LM, Ferguson SS, Daaka Y, Miller WE, Maudsley S, Della Rocca GJ, et al. Beta-arrestin-dependent formation of beta2 adrenergic receptor-Src protein kinase complexes. Science 1999;283:655–61.
43. Di Virgilio F. Purines, purinergic receptors, and cancer. Cancer Res 2012; 72:5441–7.
44. Pellegatti P, Raffaghello L, Bianchi G, Piccardi F, Pistoia V, Di Virgilio F. Increased level of extracellular ATP at tumor sites: in vivo imaging with plasma membrane luciferase. PLoS One 2008;3:e2599.
45. Morciano G, Sarti AC, Marchi S, Missiroli S, Falzoni S, Raffaghello L, et al. Use of luciferase probes to measure ATP in living cells and animals. Nat Protoc 2017;12:1542–62.
46. Khakh BS, Burnstock G. The double life of ATP. Sci Am 2009;301:84–90.
47. Jiang JX, Riquelme MA, Zhou JZ. ATP, a double-edged sword in cancer. Oncoscience 2015;2:673–4.
48. Idzko M, Hammad H, Van Nimwegen M, Kool M, Willart M, Muskens F, et al. Extracellular ATP triggers and maintains asthmatic airway inflammation by activating dendritic cells. Nat Med 2007;13:913–9.